Validation of Numerical Simulations of a Two-Span Reinforced Concrete Bridge

M. Dryden[1] and G. L. Fenves[2]

[1] *Graduate Student Researcher, Dept. of Civil and Environmental Engineering, University of California, Berkeley, USA*
Email: dryden@berkeley.edu
[2] *Professor, Dept. of Civil and Environmental Engineering, University of California, Berkeley, USA*

ABSTRACT :

Numerical simulations of the seismic response of reinforced concrete bridges must produce accurate predictions of local and global response quantities over a range of nonlinear response to facilitate performance-based earthquake engineering. Current challenges associated with these numerical simulations include selecting the column effective stiffness during the cracked-elastic response, accounting for additional flexibility at the column ends due to strain penetration along the anchored reinforcement, and modeling the column failure in flexure. To determine the efficacy of these numerical simulations, they may be validated against data from physical tests. Shake table tests of a two-span reinforced concrete bridge were conducted at the University of Nevada, Reno as part of a research effort through the Network for Earthquake Engineering Simulation (NEES). The bridge was subjected to a total of 23 ground motions in the transverse direction ranging from pre-yield and increasing until failure. These tests provide a unique opportunity to assess the validity of numerical simulations of the seismic performance of a reinforced concrete bridge over a range of nonlinear response. Nonlinear dynamic analyses of three-dimensional finite element models with different assumptions regarding the modeling of reinforced concrete columns were evaluated based on experimental data at both the local and global levels. The results of these comparisons lend insight into the implications of modeling decisions for reinforced concrete bridge systems.

KEYWORDS: bridges, finite element method, numerical models, reinforced concrete, shake table tests

1. INTRODUCTION

Existing research on the seismic performance of reinforced concrete bridge columns has focused on component tests. Such simplification has been necessary due to the limitations of testing facilities but neglects the fact that the bridge behaves as a system. Among the system effects that influence the seismic response of bridges are soil-foundation-structure interaction at the column foundations and abutments, pounding of bridge girders, and dynamic effects associated with bridge bents of differing column heights. Recent research efforts through the Network for Earthquake Engineering Simulation (NEES) have enabled researchers to collaborate by performing experimental tests and simulations at different institutions. An important NEES project involved large-scale shake table tests of a 1/4-scale, two-span reinforced concrete bridge (Johnson, et al. 2008). These tests provide a unique opportunity to validate simulations at both the global and local levels for a range of nonlinear response.

The objective of this paper is to examine and critically evaluate different assumptions for the modeling of reinforced concrete columns using two approaches: a calibrated moment-rotation model to include strain penetration effects at the column ends and a beam-column element with fixed plastic hinge lengths. The paper assesses the sensitivity of the plastic hinge lengths based on recent modeling recommendations developed using a database of column tests for the beam-column element with fixed hinge length (Berry, et al. 2008). The results from the nonlinear simulations are compared to the experimental response over a range of high-level tests. The modeling recommendations contribute to the accurate prediction of the forces and deformations in bridge systems, which is necessary for performance-based engineering design.

2. SHAKE TABLE TESTS OF A TWO-SPAN BRIDGE

Large-scale shake table tests of a 1/4-scale, two-span reinforced concrete bridge were performed at the University of Nevada, Reno. A schematic of the shake table test setup is shown in Figure 1. Differing column heights of 6 ft, 8 ft, and 5 ft were selected for bents 1, 2, and 3, respectively. The bridge design, test protocol, and measured response are described by Johnson (Johnson, et al. 2008). A series of 23 tests were conducted with table motions applied in the transverse direction only. The bridge was instrumented extensively, including displacement transducers at each bridge bent and along the heights of each column. A summary of the measured response for selected high-level shake table tests considered in this study is shown in Table 2.1. The bridge suffered significant distress in bent 3 with longitudinal reinforcement at the onset of buckling following Test 18 and significant bar buckling and fracture of the transverse spiral reinforcement occurring during Test 19.

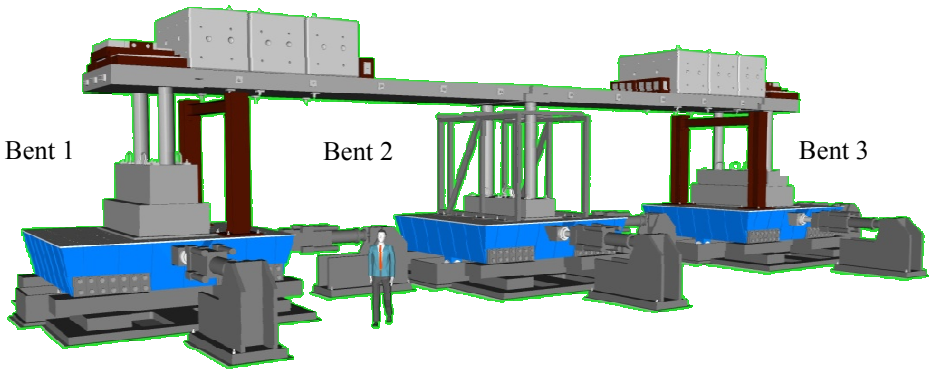

Figure 1 Shake table test setup for the two-span bridge (from Johnson, et al. 2008).

Table 2.1 Measured response for selected high-level shake table tests.

	Max Table Acceleration (g)			Max Drift Ratio (%)		
Test	Table 1	Table 2	Table 3	Bent 1	Bent 2	Bent 3
12	0.07	0.10	0.08	0.32	0.21	0.22
13	0.18	0.18	0.17	0.87	0.44	0.55
14	0.35	0.31	0.28	1.07	0.55	0.83
15	0.67	0.65	0.72	2.15	1.24	2.43
16	0.98	0.94	1.25	3.68	2.45	3.13
17	1.20	1.50	1.09	2.77	2.09	2.37
18	1.56	1.81	1.59	3.84	3.58	5.53

3. SIMULATIONS

Nonlinear dynamic analyses applying the measured table displacements were performed in OpenSees (McKenna, et al. 2000). The reinforced concrete columns were modeled by two different approaches as illustrated in Figure 2. The first approach includes a distributed plasticity element using Gauss-Lobatto quadrature with four integration points and zero-length elements at the column ends to define a moment-rotation relationship due to the strain penetration along the anchored reinforcement. Such an approach was proposed by Mazzoni (Mazzoni, et al. 2004) to account for the rigid-body rotation that occurs at the column ends as the anchored bar elongates. The moment-rotation relationship was modeled using a Hysteretic material as shown in Figure 3 with the initial assumption of a bi-uniform bond stress along the anchored bar. The bond stress distribution was assumed to be $8\sqrt{f_c'}$ and $4\sqrt{f_c'}$ for the elastic and inelastic regions, respectively, of the

anchored bar from comparisons with measured strain gauge data (Ranf 2007).

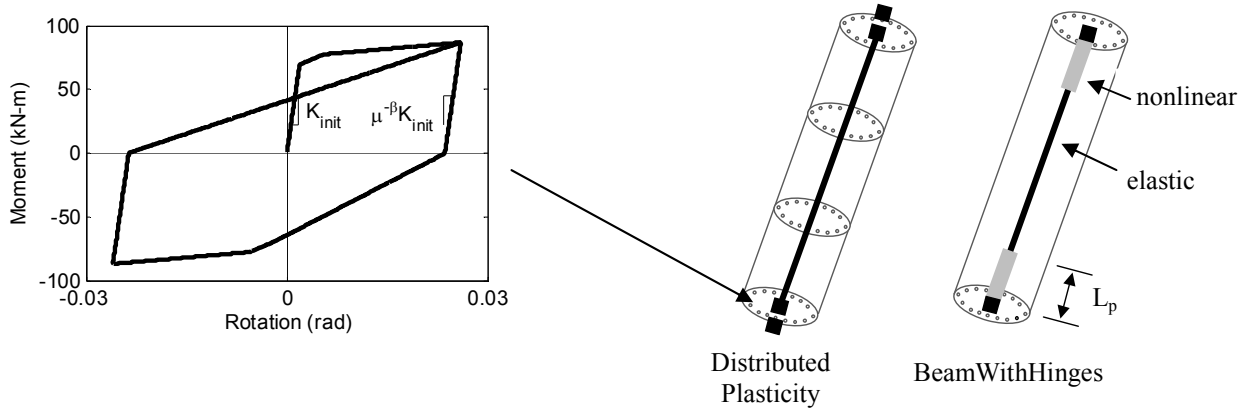

Figure 2 Column models considered in simulations.

The second approach includes a beamWithHinges (BWH) element with fixed-plastic hinge lengths at the column ends and an integration rule for the force formulation developed by Scott (Scott and Fenves 2006). Plastic hinge lengths were selected according to the relationship developed by Priestley (Priestley, et al. 1996), which includes the strain penetration effect. An effective flexural stiffness for the elastic interior of the element is defined by the point at first yield obtained from a moment-curvature analysis of the cross section. A fiber-discretized cross section is modeled using Concrete02 and a Hysteretic material for the concrete and steel, respectively, and the material model parameters are calibrated to the results of concrete cylinder and steel coupon tests. The peak stress, stress at ultimate strain, and ultimate strain for the confined concrete model are computed from the relationships developed by Mander (Mander, et al. 1988). The material models and a moment-curvature relationship for the column section are shown in Figure 3. For the purpose of describing local response, the yield curvature is defined using a bilinear approximation to the moment-curvature relationship.

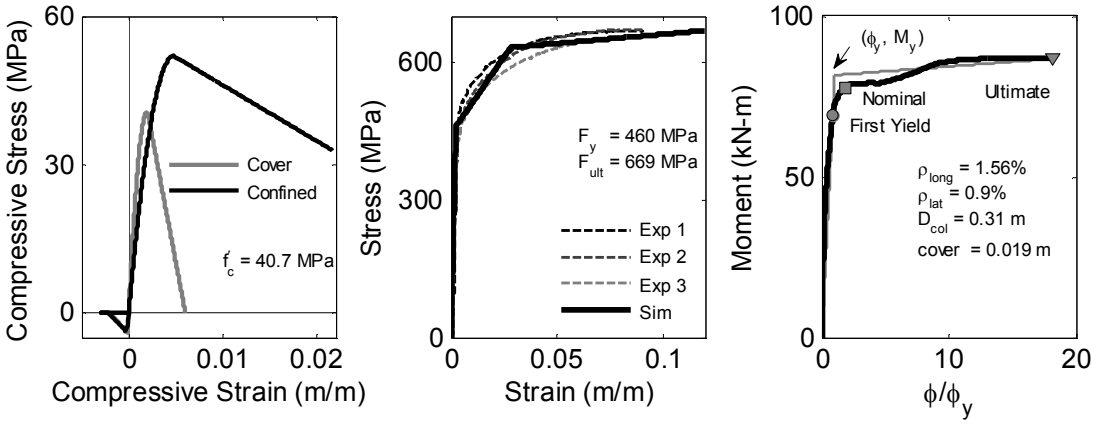

Figure 3 Material models and moment-curvature analysis of the section for all columns.

3.1. Model Calibration

The moment-rotation model representing the strain penetration effect for the first column modeling approach is calibrated using the results of the shake table tests. Two tests are selected for the calibration procedure: Test 12, where the bridge response essentially remains elastic, and Test 15, where significant yielding has taken place. The parameters varied for the low-level calibration include α, the reduction factor applied to the gross flexural

stiffness of the cap beam, and γ, the reduction factor applied to the initial stiffness of the moment-rotation model. These parameters are selected since they significantly influence the fundamental period of the simulation model, and thus its cracked-elastic response. Further calibration of the moment-rotation model for the high-level test, Test 15, is conducted by varying the parameter governing the unloading stiffness, β, and the amount of pinching in the hysteretic model. An evaluation metric (McVerry 1980) which includes the complete time history response is given by Eqn. 3.1:

$$E = \frac{\sum_{i=1}^{N}\sum_{l=l_{\min}}^{l=l_{\max}}\left|A_{\exp}^{i}(l\Delta\omega) - A_{sim}^{i}(l\Delta\omega)\right|^2}{\sum_{i=1}^{N}\sum_{l=l_{\min}}^{l=l_{\max}}\left|A_{\exp}^{i}(l\Delta\omega)\right|^2} \tag{3.1}$$

where A^{i}_{exp} and A^{i}_{sim} are the Fourier amplitudes of the displacement time histories at bent i for the experiment and simulation, respectively; N is the number of bents, l_{min} and l_{max} determine the frequency range over which the metric is calculated, and $\Delta\omega = 2\pi/T$ where T is the final time for the test under consideration. The parameters for the moment-rotation model were selected as $\alpha = 0.75$, $\gamma = 0.65$, PinchX = PinchY = 0.0, and $\beta = 0.0$ in accordance with the results of the calibration studies shown in Figure 4.

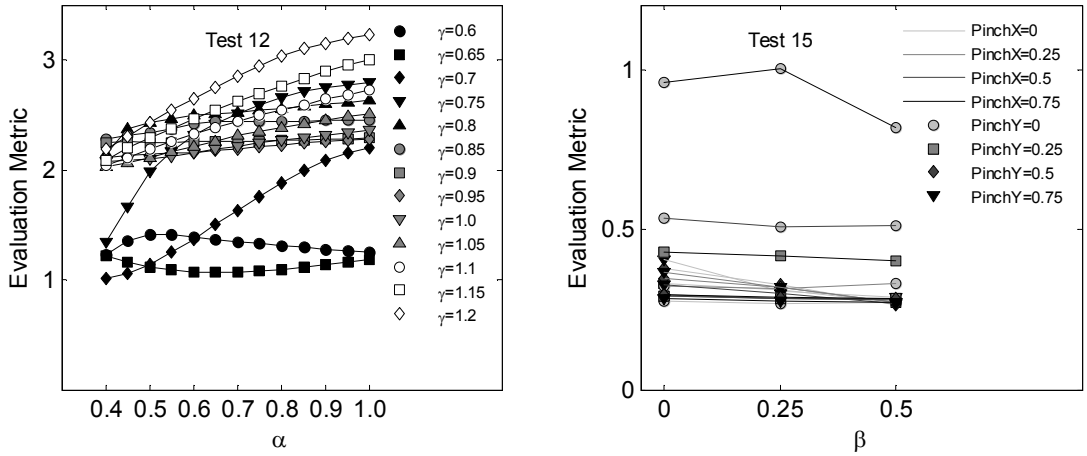

Figure 4 Variation of evaluation metric for selected modeling parameters included in the calibration study.

3.2. Validation Studies

The response of both simulation models under consideration was validated against the measured response of the two-span bridge at both the global and local levels. The simulation models are denoted as BWH for the column model with fixed plastic hinge lengths and calibrated for the column model with a calibrated moment-rotation relationship to represent the strain penetration effect. As shown in Figure 5, the two-span bridge has mode shapes for translation in the transverse direction that include twisting about bent 3, twisting about bent 2, and bending of the deck. The periods of each simulation model for these three modes are compared with results of system identification of the measured response by Ranf (Ranf 2007) in Table 3.1.

Table 3.1 Structural periods (sec) for mode shapes of the two-span bridge.

	Mode 1	Mode 2	Mode 3
BWH	0.27	0.22	0.07
Calibrated	0.33	0.25	0.07
Experiment	0.34	0.26	0.08

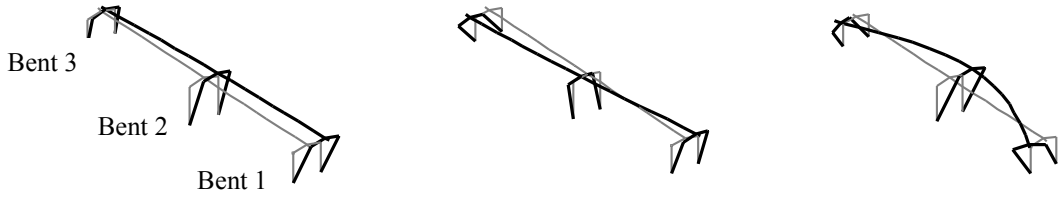

Figure 5 Mode shapes for BWH simulation model of the two-span bridge.

The bridge columns in the two-span bridge were instrumented with displacement transducers along the height of the column to measure the column curvature as shown in Figure 6. Since this instrumentation measures a rotation at a distance, h_{gauge}, away from the column ends, the curvature is computed in an average sense. As a result, this measured curvature may not reflect the true peak curvature at the column ends due to the large strain gradient that may exist at these locations. This limitation should be considered when validating the local response of the simulation model, which includes peak curvatures sampled at the element ends as shown in Figure 6. To compare the local response for the calibrated model, the curvature due to the material response at the element end, ϕ^{mat}, is added to the rotation from the adjacent zero-length element for strain penetration, θ^{SP}, divided by the length over which the displacements are measured in the experiment, h_{gauge} as given in Eqn. 3.2.

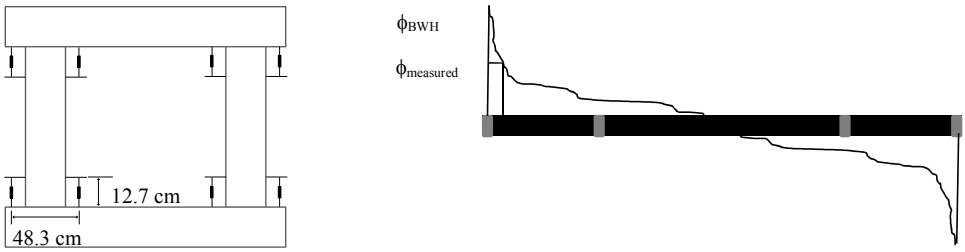

(a) (b)

Figure 6 Instrumentation for curvatures and discrepancy between curvatures from simulation and experiment.

$$\phi_{avg}^{Calibrated} = \phi^{mat} + \frac{\theta^{SP}}{h_{gauge}} \tag{3.2}$$

Selected results of the validation studies at both the global and local levels are shown for bent 3 in Figure 7. The simulation models give excellent predictions of the peak drift ratios at each bent beginning with Test 15, where significant yielding has taken place, until Test 18, at the onset of bar buckling in bent 3. For these tests, the simulations match the peak drift ratios within 20% error. Following Test 18, substantial bar buckling and fracture of the longitudinal and transverse reinforcement took place. The simulation models do not account for such phenomenon and thus cannot track the response during these final tests. The BWH model demonstrates exceptional agreement within 7% of the measured response for curvature ductilities exceeding 20 in bent 3 during Test 18. The calibrated model, which accounts for bar slip, predicts a curvature due to material response alone that is 17% less than that measured at bent 3 during Test 18. Due to the fact that the analyst typically computes curvatures from material response alone when evaluating the local response, this model underestimates the local response at levels of nonlinear deformation approaching failure. A comparison of the displacement time histories and the curvature time histories measured at bent 3 during Test 18 with those computed using the BWH simulation model is shown in Figure 8. The BWH model not only gives excellent predictions of the peak responses but also accurately tracks the entire time history response at both the global and local levels.

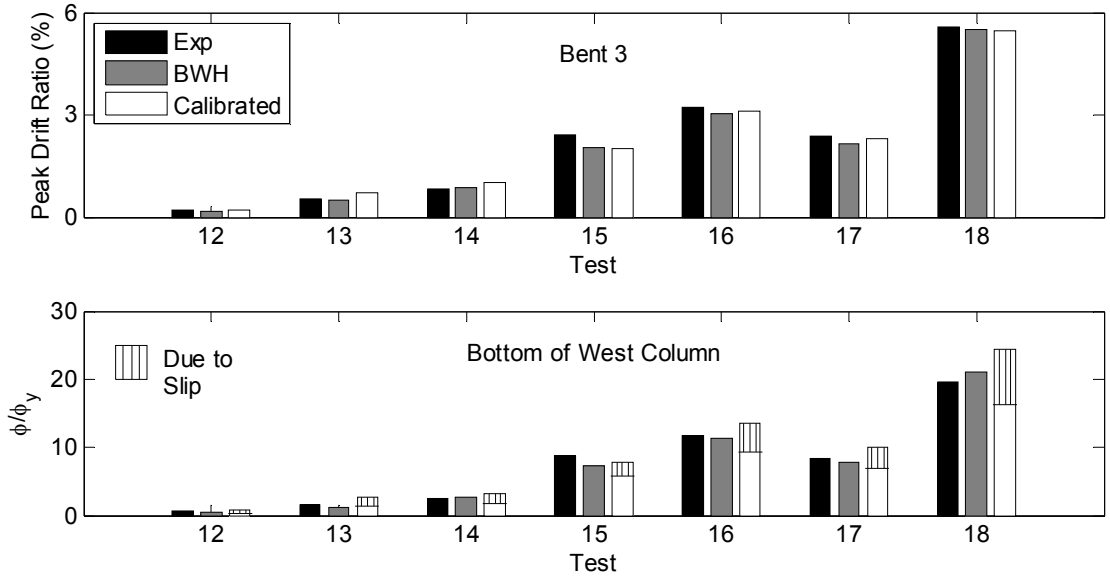

Figure 7 Comparison of peak responses at global and local levels during high-level tests.

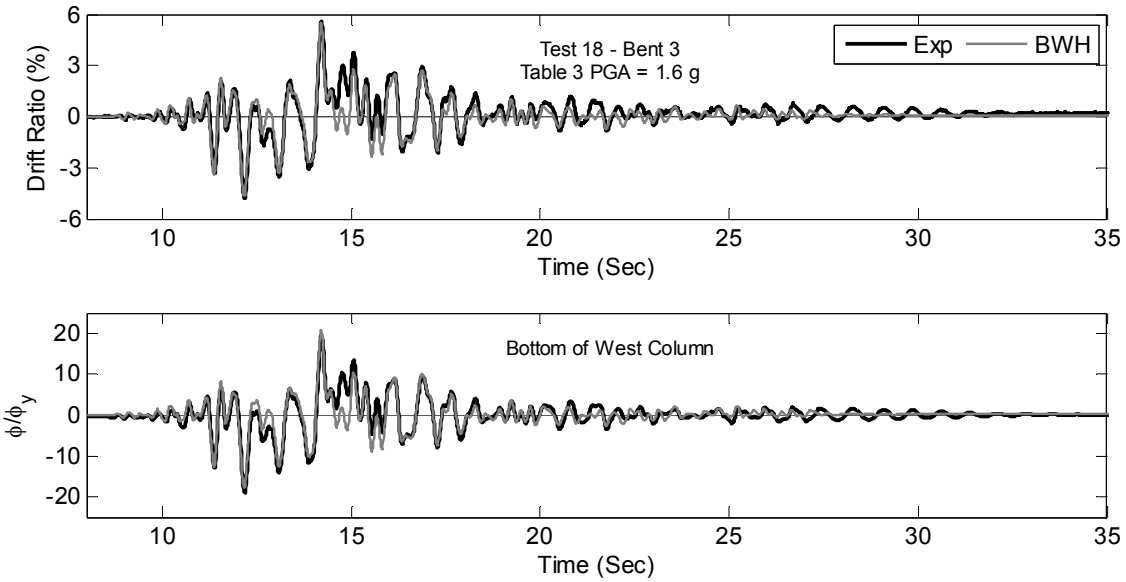

Figure 8 Comparison of time history responses at global and local levels for bent 3 during Test 18.

Additional simulations were performed to investigate the sensitivity of the response to the definition of the fixed plastic hinge length for the BWH model. Using data from 37 tests of well-detailed bridge columns, Berry proposed a relationship for the plastic hinge length based on regression analyses (Berry, et al. 2008). A comparison of the fixed plastic hinge lengths for the two modeling recommendations considered is shown in Table 3.2. As shown in Figure 9, the global response remains essentially unchanged and is irrespective of the modeling assumption for the fixed plastic hinge length. At the local level, the predicted response using the Berry model consistently overestimates that of the Priestley model with a predicted curvature 34% greater at Test 18, just prior to failure. This discrepancy highlights the sensitivity of the predicted response from simulations at levels approaching collapse to modeling assumptions for the behavior of reinforced concrete columns.

Table 3.2 Ratio of plastic hinge length to column diameter for different modeling recommendations.

	Bent 1	Bent 2	Bent 3
Priestley	0.52	0.60	0.48
Berry	0.37	0.42	0.34

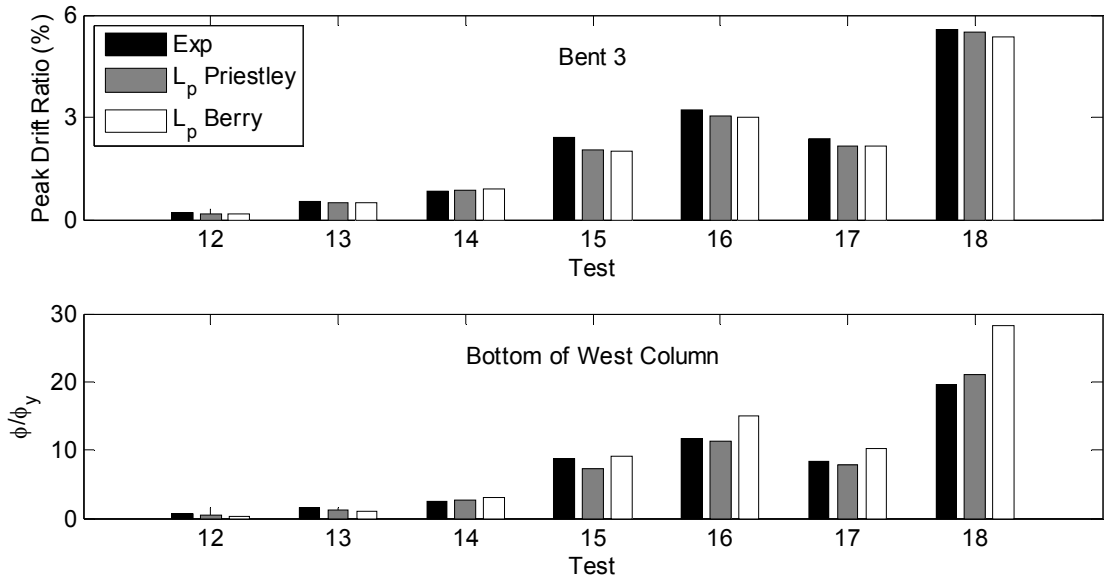

Figure 9 Comparison of peak responses for different assumptions regarding the fixed plastic hinge lengths.

4. CONCLUSIONS

Simulations of a two-span, reinforced concrete bridge using different column models have demonstrated the ability to estimate accurately the global and local response for levels approaching failure. Appropriate simplified models that incorporate degradation with increasing damage are necessary to give accurate predictions of the collapse of reinforced concrete bridges to facilitate performance-based engineering. In the absence of explicit models for aspects of failure including bar buckling, loss of confinement, and hoop fracture, the BWH model with a fixed plastic hinge length defined by Priestley matches both the local and global response well until the onset of failure. Column models employing a zero-length element at the column ends to account for strain penetration may underestimate the local response. The analyst must take care when selecting the fixed plastic hinge length for the BWH model as a shorter length may significantly impact the predicted local response.

5. ACKNOWLEDGMENTS

The research described herein is supported by the National Science Foundation through Grant No. CMS-0324343 for a NEES Demonstration Project and through a National Science Foundation Graduate Research Fellowship. The support of these funds is gratefully acknowledged. The authors would like to thank Dr. Nathan Johnson at the University of Nevada, Reno, and Dr. Tyler Ranf at the University of Washington for their work on the shake table tests of the two-span bridge. They also wish to thank Prof. Sharon Wood at the University of Texas, Austin, who served as the principal investigator for this research project.

REFERENCES

Berry, M., Lehman, D., and Lowes, L. (2008). Lumped-plasticity models for performance simulation of bridge columns. *ACI Structural Journal* **105:3**, 270-279.

Johnson, N., Ranf, R., Saiidi, M., Sanders, D. and Eberhard, M. (2008). Seismic testing of a two-span reinforced concrete bridge. *Journal of Bridge Engineering ASCE* **13:2**, 173-182.

Mander, J., Priestley, M. and Park, R. (1988). Theoretical stress-strain model for confined concrete. *Journal of Structural Engineering ASCE* **114:8**, 1804-1826.

Mazzoni, S., Fenves, G. and Smith, J. (2004). Effects of Local Deformations on Lateral Response of Bridge Frames. Technical report, University of California, Berkeley.

McKenna, F., Fenves, G., Scott, M. and Jeremic, B. (2000). Open system for earthquake engineering simulation. http://opensees.berkeley.edu.

McVerry, G. (1980). Structural identification in the frequency domain from earthquake records. *Earthquake Engineering and Structural Dynamics* **8:2**, 161-180.

Priestley, M., Seible, F. and Calvi, G. (1996). Seismic Design and Retrofit of Bridges, John Wiley & Sons, New York.

Ranf, R. (2007). Model Selection for Performance-Based Earthquake Engineering of Bridges, PhD thesis, University of Washington.

Scott, M. and Fenves, G. (2006). Plastic hinge integration methods for force-based beam-column elements. *Journal of Structural Engineering ASCE* **132:2**, 244-252.